Seismic Response Analysis of Cobble Mountain Reservoir Dam

Six finite element programs, each appropriate to a particular phase of analysis, were used instead of a single large program to predict dam behavior during an earthquake.

ALFREDO URZUA, JOHN T. CHRISTIAN, WILLIAM H. HOVER, IVAN A. HEE & STANLEY M. BEMBEN

The Cobble Mountain Reservoir Dam, located in Russell, Massachusetts, impounds the city of Springfield's primary water supply (see Figure 1). Constructed from 1929 to 1932 by hydraulic filling methods, it has a crest length of 730 feet and a maximum height of about 260 feet. The dam is a large, high-hazard structure.[1,2] It is the highest hydraulic fill dam in the world and is the highest dam in Massachusetts. Two consulting engineers were engaged as project engineers by the Springfield Water and Sewer Commission (SWSC) to evaluate the seismic stability of the dam. One was designated as the leader and all services by all of the consultants were under the lead consulting engineer's direction on behalf of the SWSC. When on-going pseudo-static analyses indicated that the dam was likely to be deemed safe, the leader promulgated a finite element dynamic analysis by a qualified consulting engineering firm. That analysis is the basis of this presentation. All contributions were included and evaluated in the project report and in a contracted version.[3,4]

The present analysis concerns the dynamic response of the embankment, evaluation of liquefaction potential and estimation of permanent deformations. Others undertook field investigations, laboratory tests, seismic hazard calculations and stability analyses. Because no available computer program can handle all the steps in the analysis, six finite element programs were used, each appropriate to one phase of the analysis. The same mesh was used for all the finite element programs. Short, special-purpose programs generated intermediate results and modified input between programs. Where the standard procedures for evaluating soil performance depend on published graphs, equivalent analytical interpolation routines were developed. Colored contours and plots of deformations made the results readily understandable. This

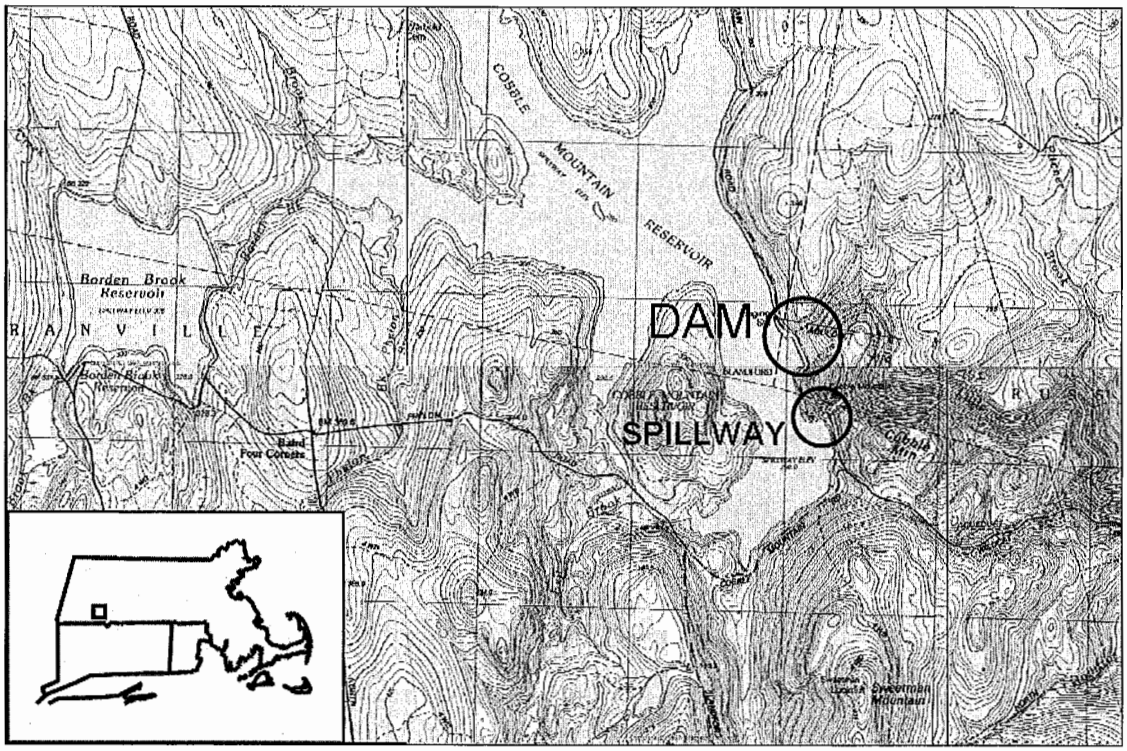

FIGURE 1. Location of Cobble Mountain Dam.

approach obviated the need to develop and debug a large computer program and provided abundant intermediate input invaluable in guiding the analysis.

Initial Conditions & Input Motions

Cross-Section & Material Properties. Figure 2 shows the central maximum cross-section of the dam. The cross-section was divided into the ten materials identified in the figure on the basis of:

- Logs of field explorations conducted in 1999;[3]
- An earlier boring program described by Roald Haested;[5]
- Laboratory and field tests during dam construction;[3] and,
- Laboratory testing with unit weights and other parameters developed and reported by Bemben and Zoino.[3]

The figure shows interpretations of the unit weight and effective friction angle for each material and also includes outlines of the finite element mesh used in the static and dynamic stress analyses. The seepage analyses used the same initial mesh, but some of the material identifications were changed. Figure 3 shows the values of the hydraulic conductivity for the various materials inferred from the results of grain size and permeability tests taken during construction and current explorations. In some later refined analyses, an eleventh material was added to represent rockfill on the upstream slope.

In addition to the properties identified on Figures 2 and 3, the analyses required that the masses and stiffnesses of the materials be established, and the liquefaction analyses required a measure of resistance of the embankment soils to liquefaction – in this case the standard penetration test N values. The masses were computed directly from the unit weights.

The stiffnesses of the various embankment materials were expressed in terms of the shear moduli, which were evaluated by a multi-step procedure. First, for each section of the dam,

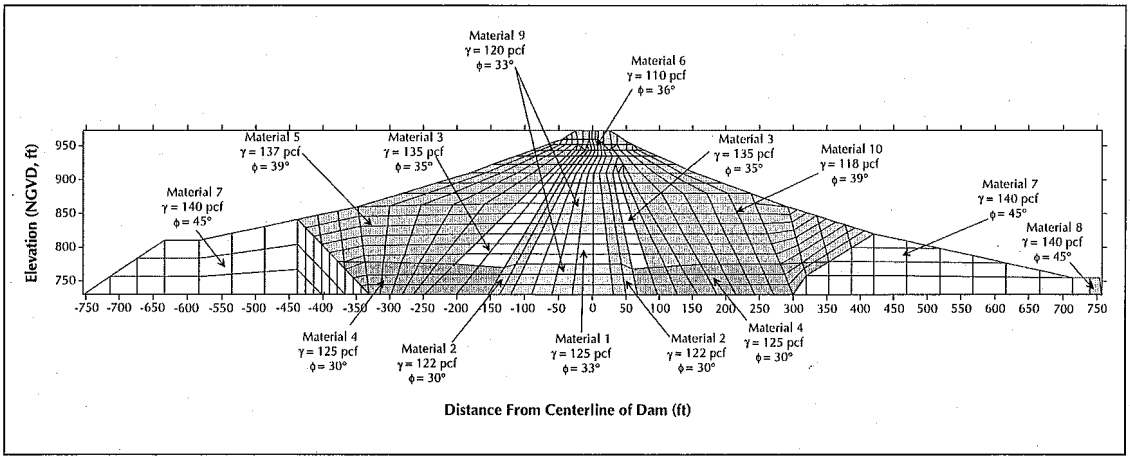

FIGURE 2. Cobble Mountain Reservoir Dam cross-section showing materials and finite element mesh for stress analyses.

the void ratio, e, was computed from the value of the unit weight, using a specific gravity of solids, G, of 2.7. The unit weight of water was taken to be 62.4 pounds per cubic foot (pcf). Next, the vertical effective stresses were estimated from the weight of overburden above the point of interest minus the pressure of water computed from the flow net described below. Values of Poisson's ratios, ν, were estimated from the results of triaxial tests, and the horizontal effective stresses were computed as the products of the vertical effective stresses and $\nu/(1-\nu)$. Poisson's ratios ranged from 0.33 for the transition zone and the bottom layer upstream of the transition zone (Materials 2 and 4) to 0.23 for the rockfill zone (Materials 7 and 8). One-third of the sum of the vertical and two horizontal effective stresses gave the octahedral stress, $\bar{\sigma}_o$. Hardin and Black gave formulas for the shear modulus of sands and clays in terms of the void ratio and the octahedral stress.[6] Seed and Idriss gave formulas for the shear modulus of gravels in terms of the octahedral stress.[7] These values are for small strain deformations, also called the "initial" modulus values. Adjusting the parameters in these formulas so that the results agreed with the available measured profiles of shear wave velocity in the field gave the following formulas for the shear moduli at small strains:[8]

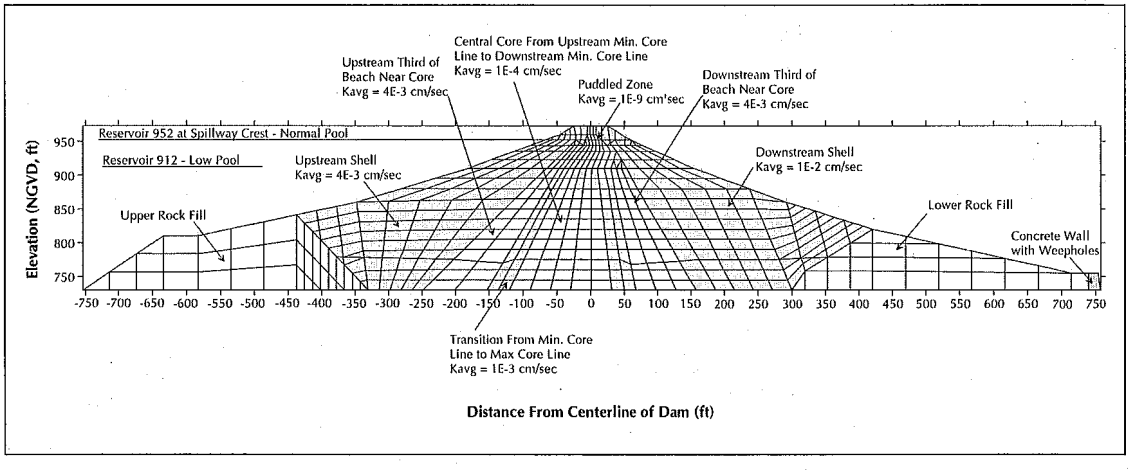

FIGURE 3. Cobble Mountain Reservoir Dam cross-section showing finite element mesh for flow analyses

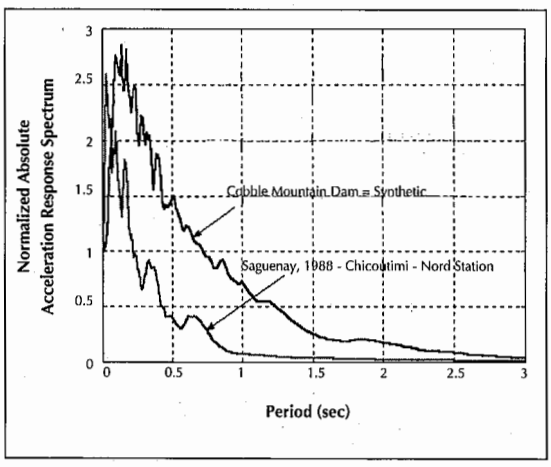

FIGURE 4. Design response spectra.

$$G = (467)\ ((2.97\text{-}e)^2/(1+e))\ \sqrt{\bar{\sigma}_o} \quad (1)$$

$$G = (3{,}795)\ \sqrt{\bar{\sigma}_o} \quad (2)$$

$$G = (998)\ ((2.17\text{-}e)^2/(1+e))\ \sqrt{\bar{\sigma}_o} \quad (3)$$

Equation 1 applies to Materials 1 and 6; Equation 2 applies to Material 7; and Equation 3 to the other materials. Both G and $\bar{\sigma}_o$ are in kips per square foot (KSF). These formulas were applied element by element to obtain an initial estimate of the distribution of shear moduli.

Conservative estimates of the standard penetration test N values were at or near the lowest values found in current explorations (correlated with energy measurements by Heller and Johnsen, and the corrected values by Bemben-Zoino study[3]). For the gravels in Material 7, N was taken to be 25. For the core Materials 1 and 9, N was taken to be 8, which is increased from 7 because the tests had higher than usual energy transmission. For Material 2, N was taken to be 12. For all the other materials an N value of 15 was used.

Earthquake Records. A probabilistic seismic hazard analysis was conducted in 2000 and yielded two possible design earthquakes for incorporation into the seismic analysis.[9] One was a synthetic record developed conservatively for this project, called the "Cobble Mountain Synthetic Earthquake." The other was one of the actual records of the 1988 magnitude 5.8 Saguenay earthquake at Chicoutimi-Nord Station, Québec. Each of these earthquakes were scaled to peak base accelerations (PBA) of 0.12 g and 0.16 g to reflect different levels of earthquake magnitudes, corresponding to recurrence intervals of about 6,000 years and 10,000 years, respectively. The Chicoutimi-Nord earthquake was also scaled to 0.204 g to represent an event similar to that considered by others for the Knightville Dam.[10] The project engineers selected the synthetic earthquake with a PBA of 0.16 g and the actual record earthquake with a PBA of 0.204 g as the two design cases. (The Knightville Dam is about 12 miles to the north-northeast of the Cobble Mountain Dam.) The shapes of the acceleration spectra for 5 percent damping for the records normalized to 1.00 g are displayed in Figure 4.

Initial Effective Stress Conditions. To calculate the *in situ* initial effective stress conditions, the total vertical stresses were first computed with the finite element program SIGMA/W using total unit weights.[11] Figure 5 shows the contours of vertical total stress for the reservoir at full pool (spillway crest at elevation 952 — datum is National Geodetic Vertical Datum [NGVD]), and Figure 6 shows the contours for the reservoir at low pool (ele-

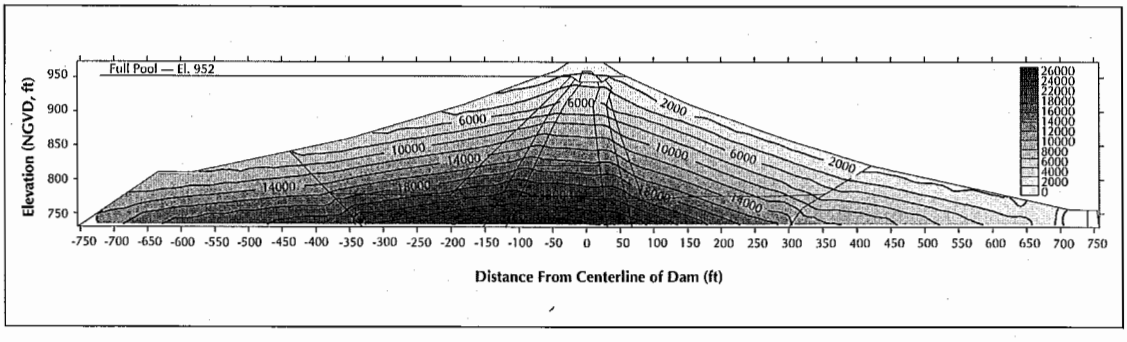

FIGURE 5. Initial total vertical stresses at full pool.

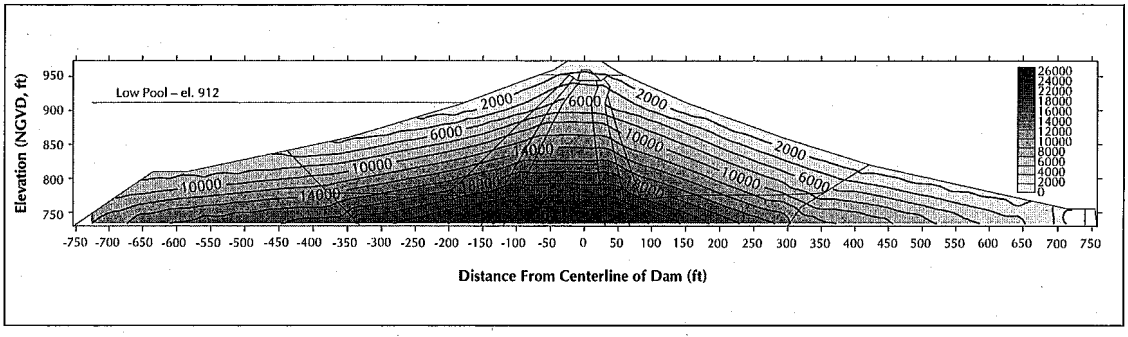

FIGURE 6. Initial total vertical stresses at low pool.

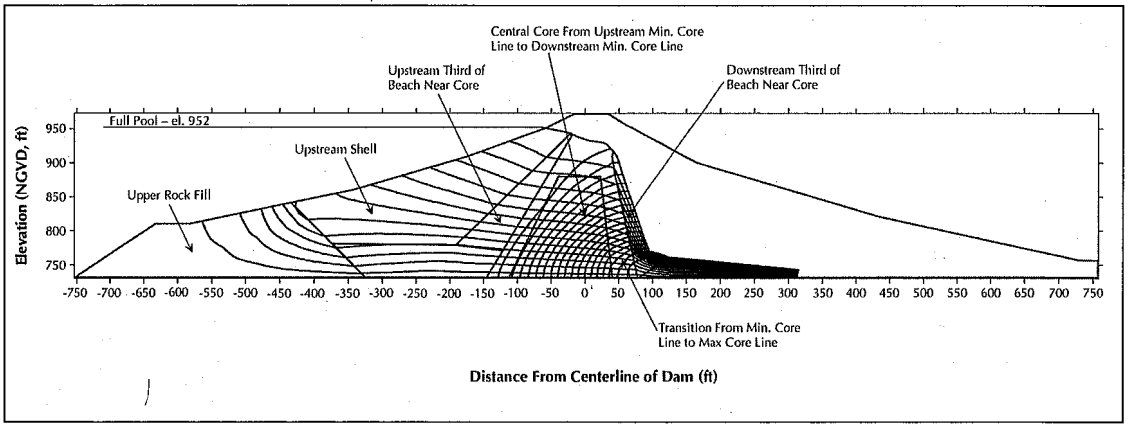

FIGURE 7. Flow net at full pool.

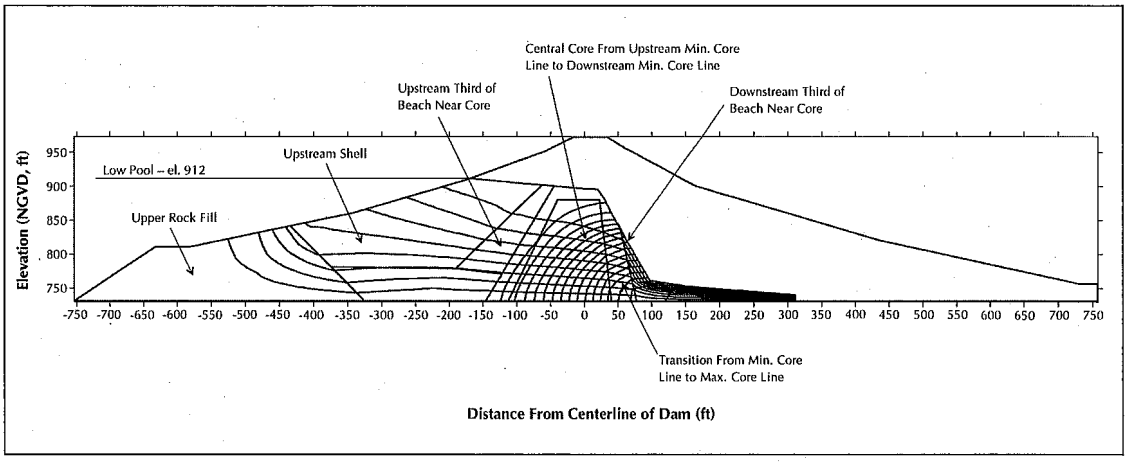

FIGURE 8. Flow net at low pool.

vation 912, or 40 feet lower than full pool). The seepage regime was evaluated using two finite element programs: SEEP/W[12] and a proprietary program that could plot the full flow net (seepage flow lines as well as the equipotentials) using Christian's method.[13] Seepage was evaluated for the reservoir at elevation 952 feet (full pool) and at elevation 912 feet (low pool). Figures 7 and 8 show the flow nets for the two conditions. Finally, the pore pressures found from the SEEP/W analyses were subtracted from the total vertical stresses to

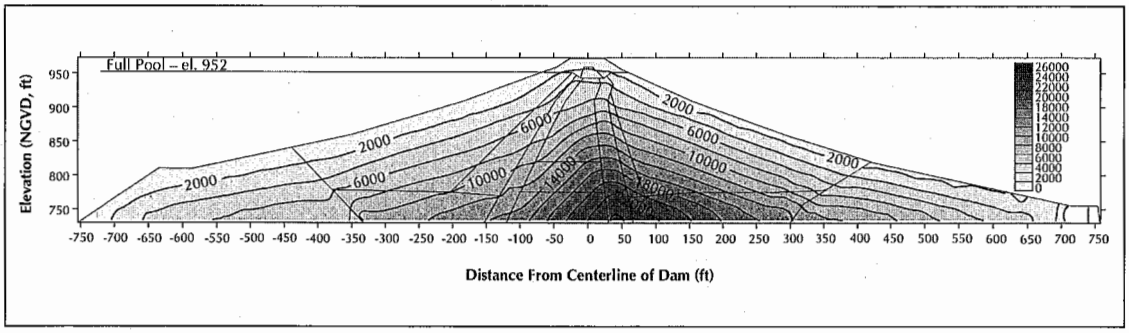

FIGURE 9. Initial effective vertical stresses at full pool.

give the effective vertical stresses plotted in Figures 9 and 10.

Response Analysis Methodology

The response of an embankment to seismic shaking is a complicated process involving many phenomena. In an ideal world there would be one or two computer systems that could accommodate the full range of behavior and geometry, but that is not now the case. Furthermore, the elaborate systems that do exist are relatively inflexible and hard to adapt to specific conditions. Therefore, it was decided to proceed with several proven analytical tools and to do so in a way that intermediate results could be conveniently transmitted from one finite element program to another. An essential component of this approach was the decision to maintain one finite element mesh.

Two-Dimensional Analysis. Two computer programs were selected to perform the dynamic analysis: QUAD-4M and FLUSH. The QUAD-4M model works in the time domain — *i.e.,* the effects of the earthquake motion input at the bedrock foundations at the base of the dam are calculated one time step at a time throughout the record.[14] The FLUSH model works in the frequency domain — *i.e.,* it first performs a fast Fourier transform on the earthquake record to obtain Fourier amplitudes at different frequencies, solves the response at each frequency and then transforms the results back into the time domain.[15] Both programs evaluate the maximum shear stress in each element and use 65 percent of these values to calculate the appropriate strain-dependent values of modulus and damping for each element. Furthermore, since both models were expected to produce generally similar results, using two models in some ways helped provide a check of accuracy input. The present analysis employed the modulus and damping curves developed by Vucetic and Dobry.[16] The results of the analyses were values of horizontal shear strains and shear stresses at the centroid of each finite element in the 522-element mesh. The models also yielded internal accelerations and peak volumetric strains within the dam as a result of the base excitation. QUAD-4M consistently gave slightly higher responses than

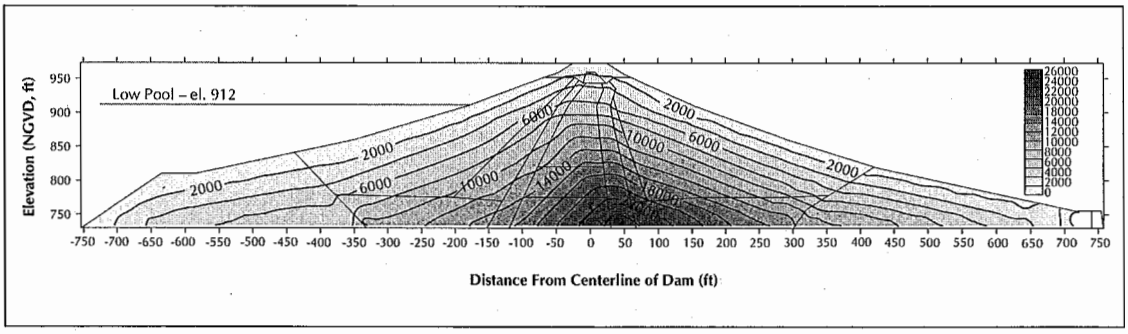

FIGURE 10. Initial effective vertical stresses at low pool.

FLUSH for the 0.12 g and 0.16 g earthquakes. Therefore, only QUAD-4M was used for the later analyses at 0.204 g.

Pseudo-Three-Dimensional Analyses. The two-dimensional analyses assume that the dam is a prism extending infinitely perpendicular to the plane of the cross-section (*i.e.*, along the long axis of the dam). In fact, the length of the dam between abutments is less than the distance from toe to toe at the maximum section. The ratio of length to height of the longitudinal distance or crest length, L, to the maximum height, H, is 3 for the Cobble Mountain Dam. Makdisi *et al.* proposed a procedure for making the necessary corrections for three-dimensional effects.[17] They reported that, for L/H equal to 3, the ratio of the fundamental frequency under three-dimensional conditions to that computed for two-dimensional conditions is 1.6. This ratio is designated R_f. The iterated two-dimensional final fundamental period given by the QUAD-4M or FLUSH is T_{2D}. Then, the three-dimensional fundamental period T_{3D} is equal to T_{2D} divided by R_f. For a particular response spectrum the spectral acceleration at T_{3D} is Sa_{3D}. The spectral acceleration at T_{2D} is Sa_{2D}. Then R_{Sa} is equal to Sa_{3D} divided by Sa_{2D} (the ratio of the three-dimensional to the two-dimensional spectral acceleration) and R_{Sd} is equal to R_{Sa} divided by the square of R_f (the ratio of the spectral displacements). A simple program was written to read the output of the two-dimensional analyses and compute this ratio for each element. The iterated fundamental period computed in the two-dimensional analyses varied with the level of shaking, the computer program that was used and the time history, but values generally fell between 1.1 and 1.3 seconds.

For a particular element from the QUAD-4M or FLUSH results, the two-dimensional effective horizontal shear strain is $\gamma_{xy,eff}$ (65 percent of the maximum value). The new effective shear strain, $\gamma_{xy,eff,\ new}$, is equal to $\gamma_{xy,eff}$ times R_{Sd}. For $\gamma_{xy,eff,\ new}$, the Dobry-Vucetic curves give a new value of shear modulus, G_{new}. The new value of the effective cyclic shear stress, $\tau_{eff,\ new}$, is equal to G_{new} times $\gamma_{xy,eff,\ new}$. The new value of the cyclic shear stress, $\tau_{eff\ new}$, can then be used in the calculations of settlement and factors of safety against liquefaction.

Liquefaction Analysis. Liquefaction analysis compares the horizontal shear stresses generated by the earthquake with the resistance available to prevent liquefaction. The shear stresses are expressed in terms of a cyclic stress ratio (CSR), and the resistance in terms of a cyclic resistance ratio (CRR). The procedures used here are those proposed by the 1996 National Center for Earthquake Engineering (NCEER) and 1998 NCEER/National Science Foundation Workshops, which represent the latest consensus on the state of practice.[18]

The CSR is equal to 65 percent of the ratio of the peak horizontal shear stress generated by the earthquake to the initial vertical effective stress:

$$CSR = 0.65 \bullet \tau_{peak}/\bar{\sigma}_{v,init} \quad \textbf{(4)}$$

The factor of 0.65 represents an averaging over the time history. The CRR is found from a plot of CRR versus the standard penetration test N value corrected for 60 percent energy efficiency and for a vertical effective stress of 1 ton per square foot (or, $(N_1)_{60}$). The plot is found in Youd *et al.*, but it is based on a series of publications by Seed and his co-workers dating back to the 1970s.[18] Except as noted above, the N values found in the field exploration program generally represent 60 percent energy efficiency. The correction for the vertical effective stress is achieved by multiplying the N value by C_N (which is equal to $(2{,}000/\sigma_{v,init})^{1/2}$), where the stresses are in psf. It is also necessary to correct for a fines content larger than 5 percent. This correction is done using the formula:

$$(N_1)_{60,\ corrected} = \alpha + \beta \bullet (N_1)_{60,\ uncorrected} \quad \textbf{(5)}$$

This correction is necessary only for the material in the core, where α is equal to 5 and β is equal to 1.2.

The factor of safety against liquefaction is then computed from:

$$FS = (CRR/CSR) \bullet MSF \bullet K_\sigma \bullet K_\alpha \quad \textbf{(6)}$$

MSF is a magnitude-scaling factor to account for the fact that the magnitude at which the

empirical factors were calibrated is 7.5. In the present case, with the three levels of acceleration, the MSF was 1.75, 1.7 and 1.5 for the 0.12 g, 0.16 g and 0.204 g earthquakes, respectively. K_σ varies between 1.7 and 0.5 as a function of the overburden stress according to charts presented by Youd *et al.*[18] K_α is difficult to estimate; it was assumed conservatively to be 1.0.

Estimated Strains & Settlement. The output from both the QUAD-4M and FLUSH programs includes peak values of shear strain during the earthquake. For soils above the phreatic surface, Tokimatsu and Seed gave relations between the volumetric strain, the peak shear strain and N value.[19] For each element above the phreatic surface, the peak shear strain computed from the dynamic finite element analysis and the N value at that point were entered into the Tokimatsu and Seed relations to yield the volumetric strain. For saturated soils beneath the phreatic surface, Ishihara and Yoshimine gave relations for the volumetric strain as a function of the factor of safety against liquefaction and the N value.[20] (The relation is in the form of a chart that is also found in Ishihara's book.[21]) For each element below the phreatic surface, the factor of safety against liquefaction and the N value were entered into the Ishihara and Yoshimine relation to obtain the volumetric strain. The results of the Tokimatsu and Seed and the Ishihara and Yoshimine computations are unconstrained volumetric strains in the sense that they do not account for the restraining effect of adjacent elements.

Both the Tokimatsu and Seed and the Ishihara and Yoshimine relations are in the form of charts, which cannot be used directly in a computerized, element-by-element analysis. Therefore, second-order regression analyses were run using the points in the charts to obtain analytical forms appropriate for interpolation. The Ishihara and Yoshimine chart had to be divided into three sections to obtain adequate resolution.

The unconstrained volumetric strains were then used as input conditions to a general-purpose finite element program, PC-FEAP.[22] This program redistributed the displacements to restore continuity, yielding a deformed continuous mesh and a settlement profile of the top of the dam along the maximum section.

Major Results

The dam was analyzed in order of increasing level of peak base acceleration at the top of bedrock – 0.12 g, 0.16 g and 0.204 g. The results include contours of factor of safety against liquefaction, deformed meshes showing the effect of volume change following the earthquake and estimated settlement profiles for the top surface of the dam along the maximum section. Each of these three levels of shaking describes results that include the effects of the three-dimensional corrections. However, in order to demonstrate the relative contributions of various parameters, the results of the 0.12 g peak base acceleration includes a description of the two-dimensional results as well.

Peak Base Acceleration – 0.12 g. Figures 11 through 14 display the contours of the factor of safety against liquefaction for the reservoir at full pool when it is shaken by earthquakes with a peak base acceleration of 0.12 g in the bedrock surface beneath the dam. The four figures include all combinations of two time histories (Cobble Mountain synthetic record and the Chicoutimi-Nord record) and two methods of analysis (QUAD-4M and FLUSH). The results are for two-dimensional analyses with no corrections for the upstream slope rockfill zone effects. The results demonstrate that the most severe of the four cases is that of the Cobble Mountain synthetic record analyzed with QUAD-4M. The minimum value of the factor of safety was 1.25, located within the 1.5 contour in Figures 11 and 12.

The deformed mesh in Figure 15 shows the shape of the dam after the volumetric strains induced by the 0.12 g earthquake shaking have been accounted for. The deformations are exaggerated 25-fold. These results are from a two-dimensional analysis using QUAD-4M and the Cobble Mountain synthetic record.

For the case of reservoir at the low pool level, Figures 16 through 19 show the corresponding contours of the factors of safety against liquefaction. Figure 20 shows the deformed mesh. Again, the deformations are exaggerated by a factor of 25, and these results are also for two-dimensional analyses.

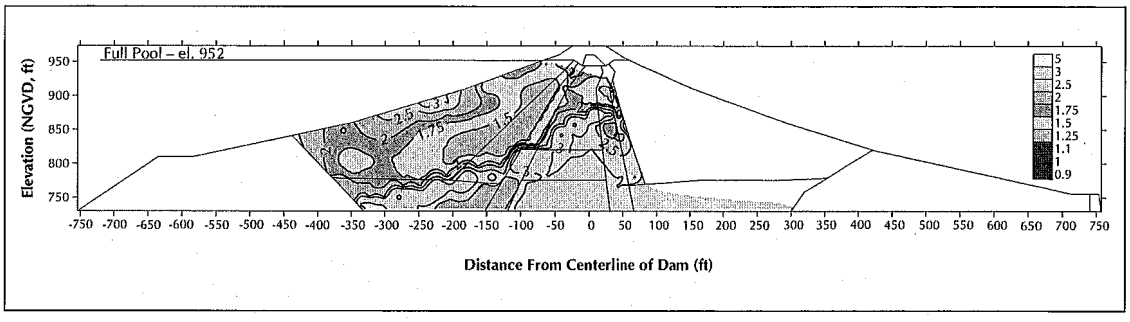

FIGURE 11. Factors of safety against liquefaction, Cobble Mountain synthetic earthquake, QUAD-4M analysis, peak base acceleration 0.12 g, full pool, two-dimensional analysis.

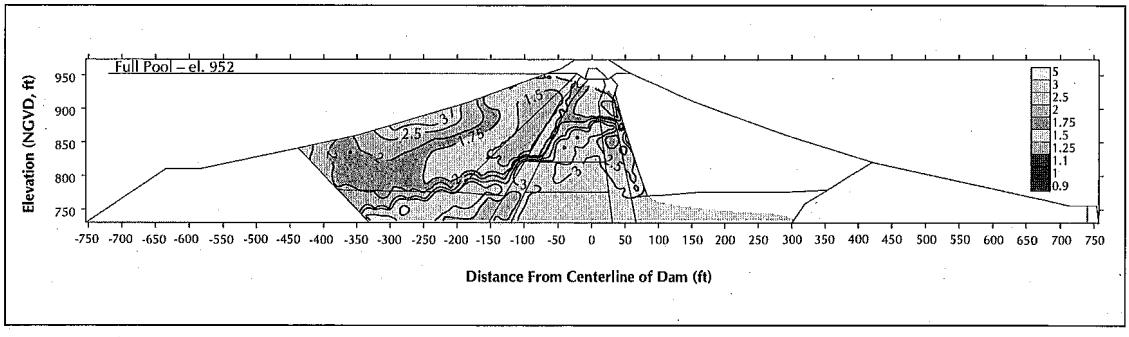

FIGURE 12. Factors of safety against liquefaction, Cobble Mountain synthetic earthquake, FLUSH analysis, peak base acceleration 0.12 g, full pool, two-dimensional analysis.

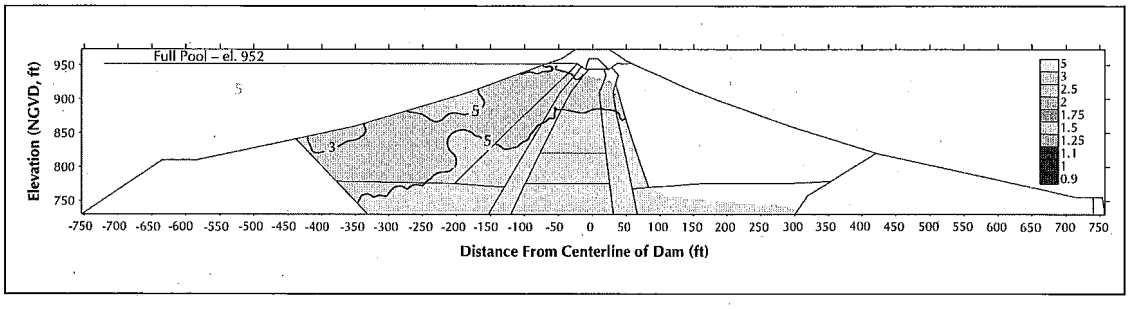

FIGURE 13. Factors of safety against liquefaction, Chicoutimi-Nord record, QUAD-4M analysis, peak base acceleration 0.12 g, full pool, two-dimensional analysis.

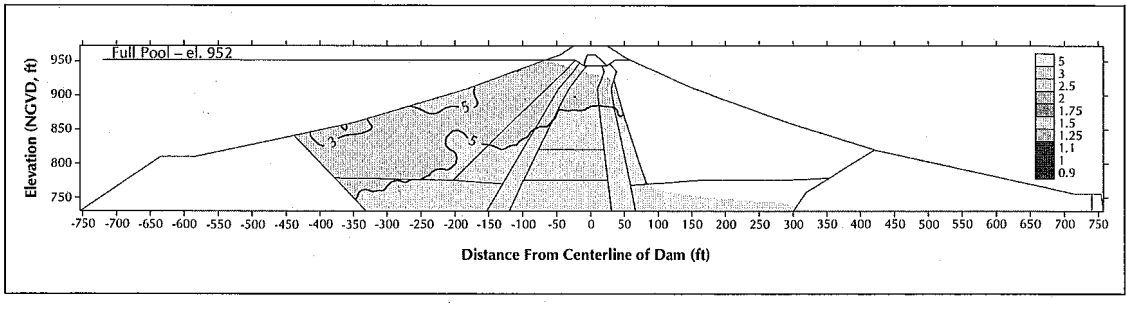

FIGURE 14. Factors of safety against liquefaction, Chicoutimi-Nord record, FLUSH analysis, peak base acceleration 0.12 g, full pool, two-dimensional analysis.

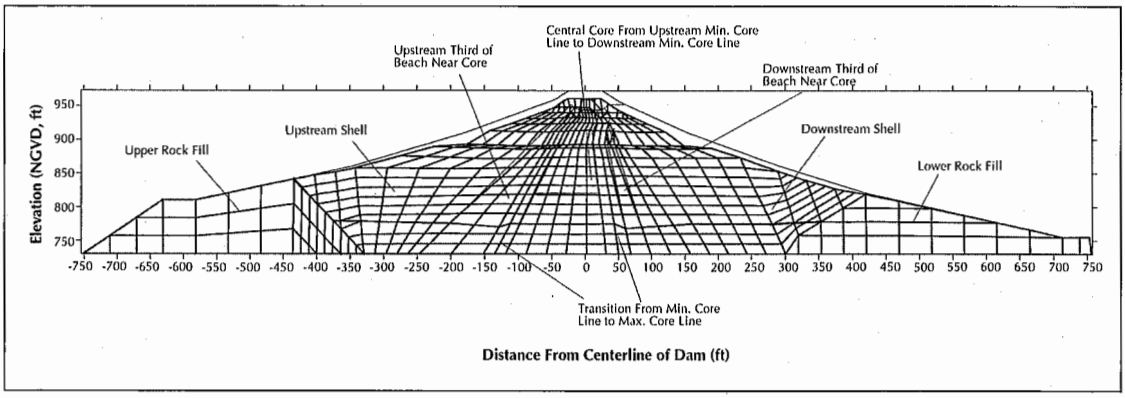

FIGURE 15. Deformed mesh (25-fold exaggeration), Cobble Mountain synthetic earthquake, QUAD-4M analysis, peak base acceleration 0.12 g, full pool, two-dimensional analysis.

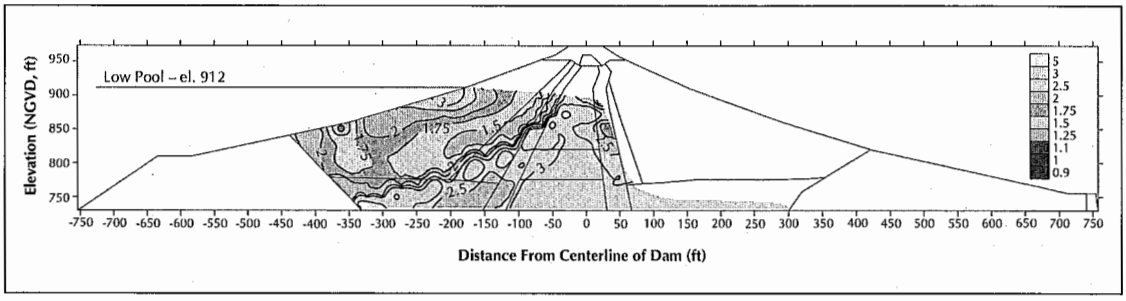

FIGURE 16. Factors of safety against liquefaction, Cobble Mountain synthetic earthquake, QUAD-4M analysis, peak base acceleration 0.12 g, low pool, two-dimensional analysis.

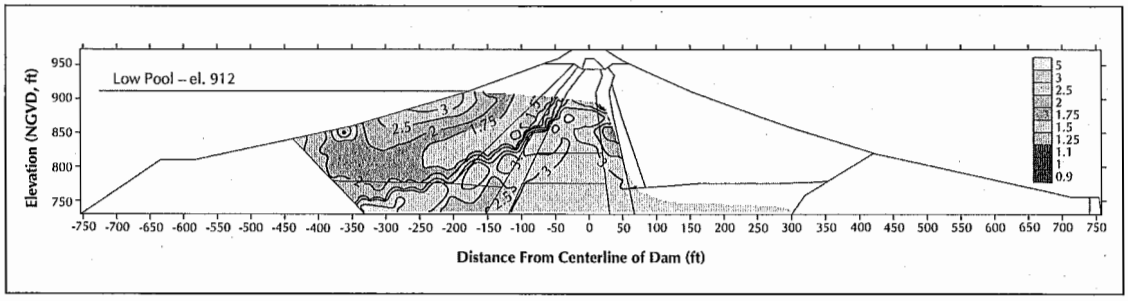

FIGURE 17. Factors of safety against liquefaction, Cobble Mountain synthetic earthquake, FLUSH analysis, peak base acceleration 0.12 g, low pool, two-dimensional analysis.

Figure 21 is a plot of the estimated final settlement of the top of the dam in the two-dimensional analyses. Six cases are plotted: full and low pool for 0.12 g, and full and low pool for 0.16 g with and without upstream rockfill modeled. In all cases, the results are for the Cobble Mountain synthetic record and the QUAD-4M program. When the three-dimensional corrections are made for the case of full pool, the contours of factor of safety against liquefaction become those that are shown in Figure 22. This figure uses the results of QUAD-4M analysis with the Cobble Mountain synthetic record normalized to 0.12 g. The factors of safety for the Chicoutimi-Nord record at 0.12 g are contoured in Figure 23. The deformed mesh, with deformations exaggerated by a factor of 25, is plotted in Figure 24 for the Cobble Mountain synthetic record and in Figure 25 for the Chicoutimi-

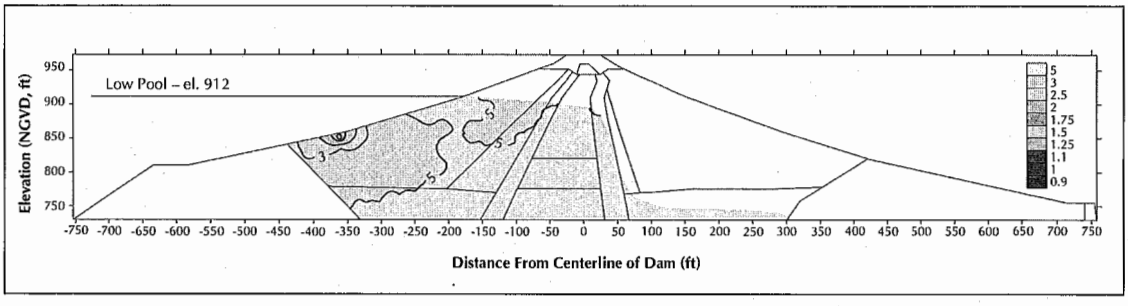

FIGURE 18. Factors of safety against liquefaction, Chicoutimi-Nord record, QUAD-4M analysis, peak base acceleration 0.12 g, low pool, two-dimensional analysis.

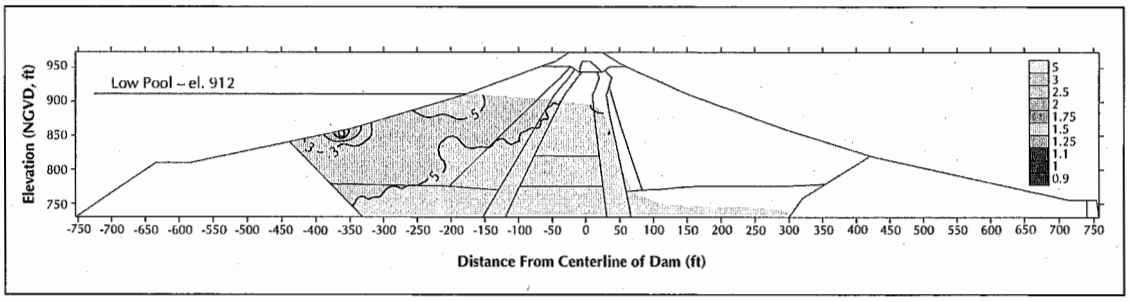

FIGURE 19. Factors of safety against liquefaction, Chicoutimi-Nord record, FLUSH analysis, peak base acceleration 0.12 g, low pool, two-dimensional analysis.

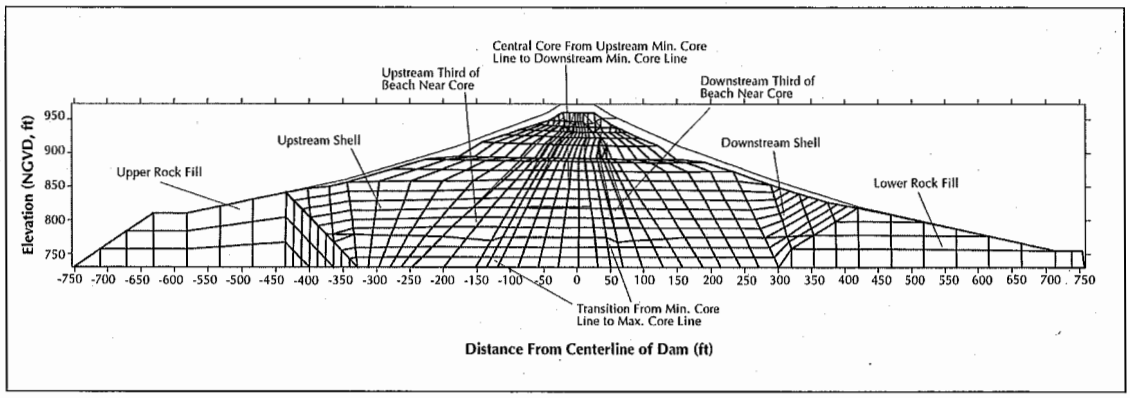

FIGURE 20. Deformed mesh (25-fold exaggeration), Cobble Mountain synthetic earthquake, QUAD-4M analysis, peak base acceleration 0.12 g, low pool, two-dimensional analysis.

Nord record. Both records were normalized to 0.12 g, and the analyses were done with QUAD-4M.

Figure 26 shows the settlement of the top surface corrected for three-dimensional effects. It corresponds to Figure 21 for the two-dimensional case. Figure 26 is for the Cobble Mountain synthetic record and QUAD-4M analysis. It also includes the results for 0.16 g input.

Peak Base Acceleration – 0.16 g. Figure 27 presents the contours of the factor of safety against liquefaction at full pool, including three-dimensional effects, for the QUAD-4M analysis with the Cobble Mountain synthetic record normalized to 0.16 g. The factors of safety for the Chicoutimi-Nord record at 0.16 g are contoured in Figure 28. The deformed mesh for full pool, with deformations exaggerated by a factor of 25, is plotted

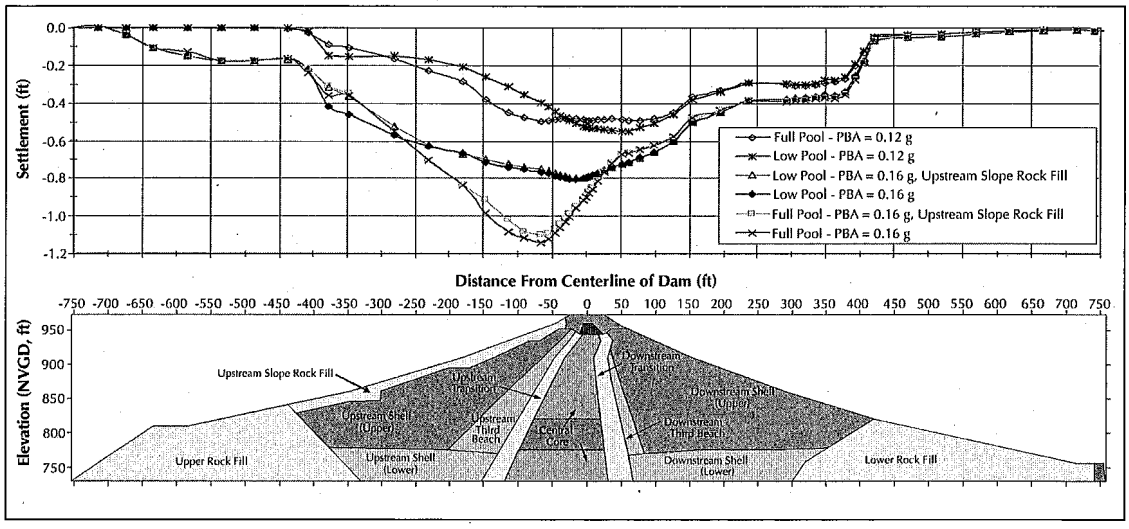

FIGURE 21. Estimated settlement along the top surface of the profile, two-dimensional QUAD-4M analysis, Cobble Mountain synthetic earthquake.

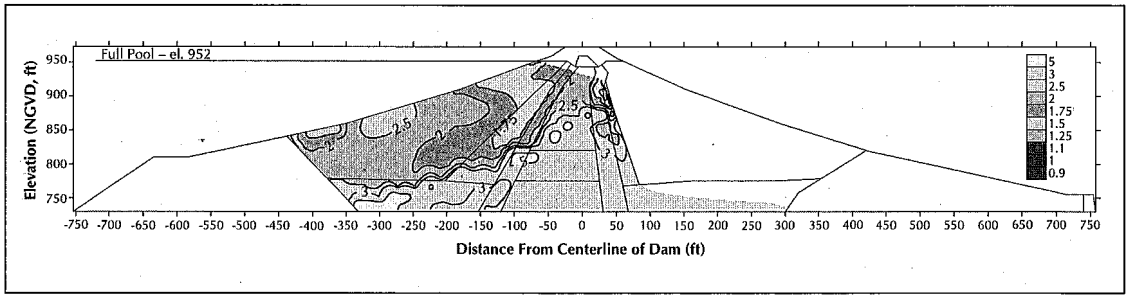

FIGURE 22. Factors of safety against liquefaction, Cobble Mountain synthetic earthquake, QUAD-4M analysis, peak base acceleration 0.12 g, full pool, pseudo-three-dimensional analysis.

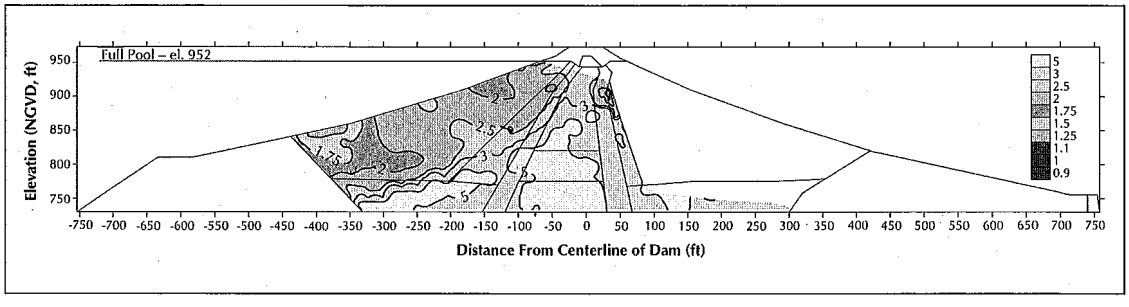

FIGURE 23. Factors of safety against liquefaction, Chicoutimi-Nord record, QUAD-4M analysis, peak base acceleration 0.12 g, full pool, pseudo-three-dimensional analysis.

in Figure 29 for the Cobble Mountain synthetic record.

The pseudo-three-dimensional analyses show that when the reservoir is at low pool, the factors of safety are similar and the deformations are less. However, in localized shallow zones beneath the upstream slope of the dam, where effective confining stresses are relatively low, initial computed factors of safety were as low as 0.9 to 1.0. These low values are artifacts of a conservative decision originally not to model the beneficial effects of the

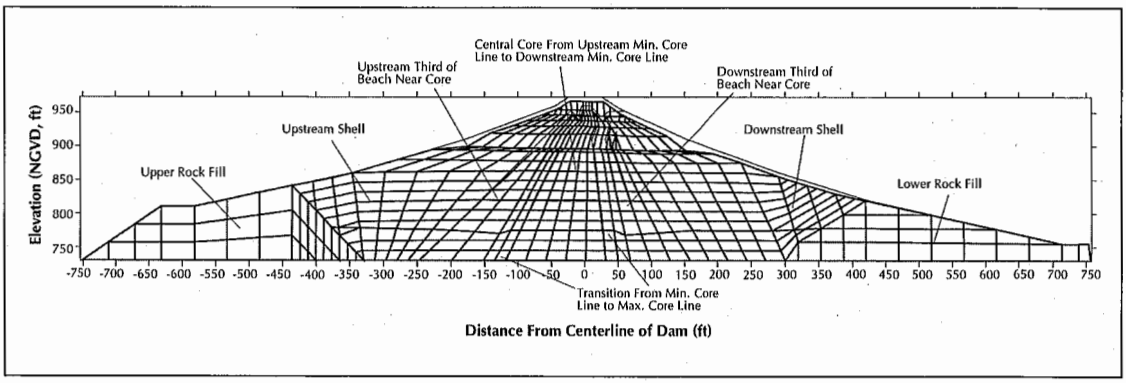

FIGURE 24. Deformed mesh (25-fold exaggeration), Cobble Mountain synthetic earthquake, QUAD-4M analysis, peak base acceleration 0.12 g, full pool, pseudo-three-dimensional analysis.

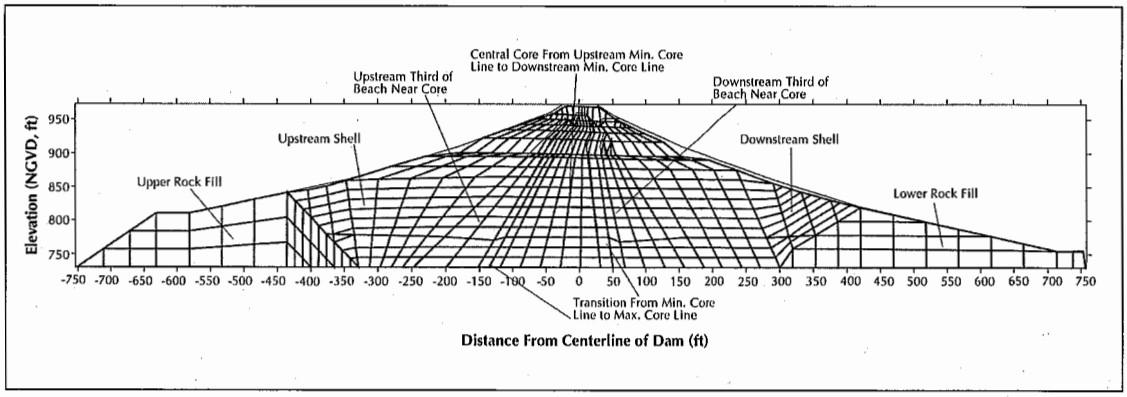

FIGURE 25. Deformed mesh (25-fold exaggeration), Chicoutimi-Nord record, QUAD-4M analysis, peak base acceleration 0.12 g, full pool, pseudo-three-dimensional analysis.

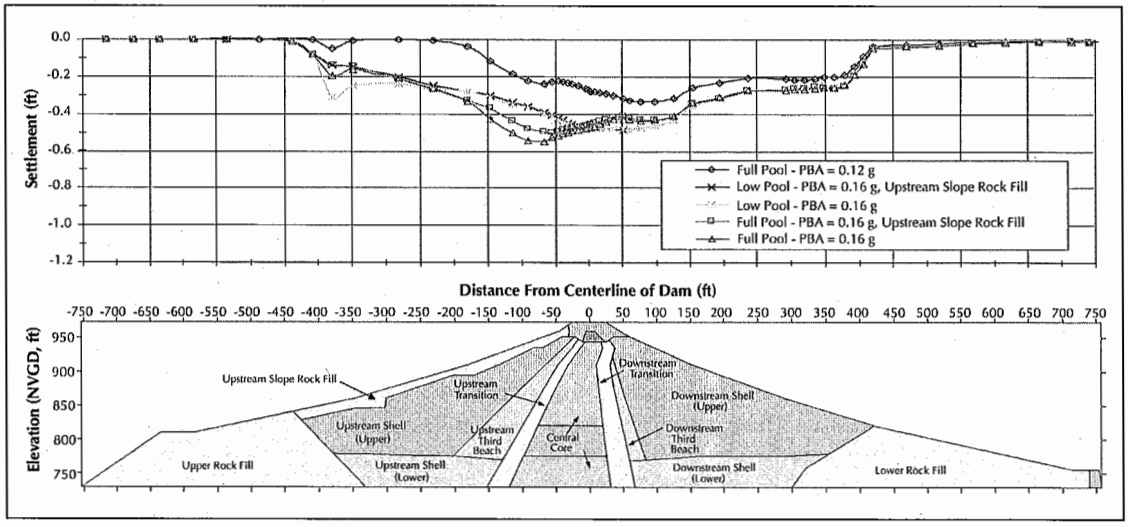

FIGURE 26. Estimated settlement along the top surface of profile, pseudo-three-dimensional QUAD-4M analysis, Cobble Mountain synthetic earthquake, full and low pool, 0.12 g and 0.16 g peak base accelerations.

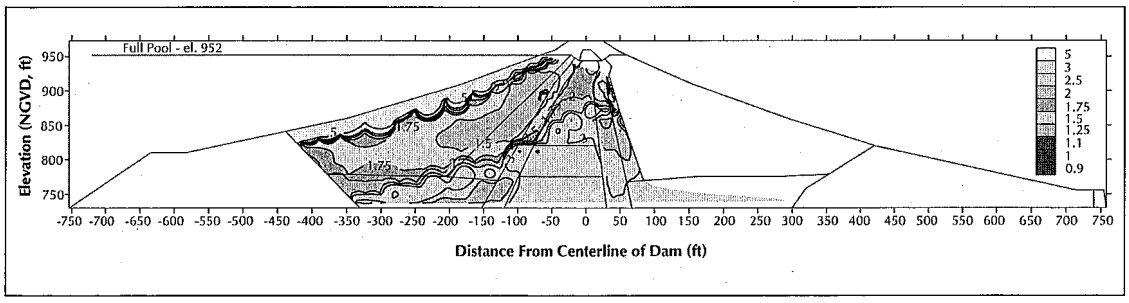

FIGURE 27. Factors of safety against liquefaction, Cobble Mountain synthetic earthquake, QUAD-4M analysis, peak base acceleration 0.16 g, full pool, upstream slope rockfill pseudo-three-dimensional analysis.

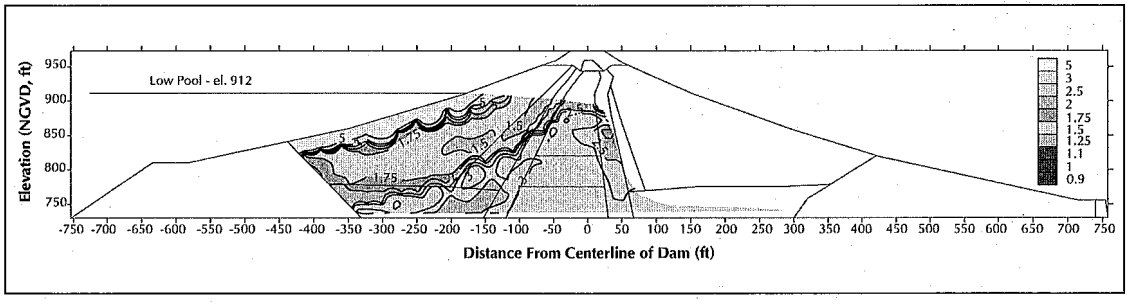

FIGURE 28. Factors of safety against liquefaction, Cobble Mountain synthetic earthquake, QUAD-4M analysis, peak base acceleration 0.16 g, low pool, upstream slope rockfill pseudo-three-dimensional analysis.

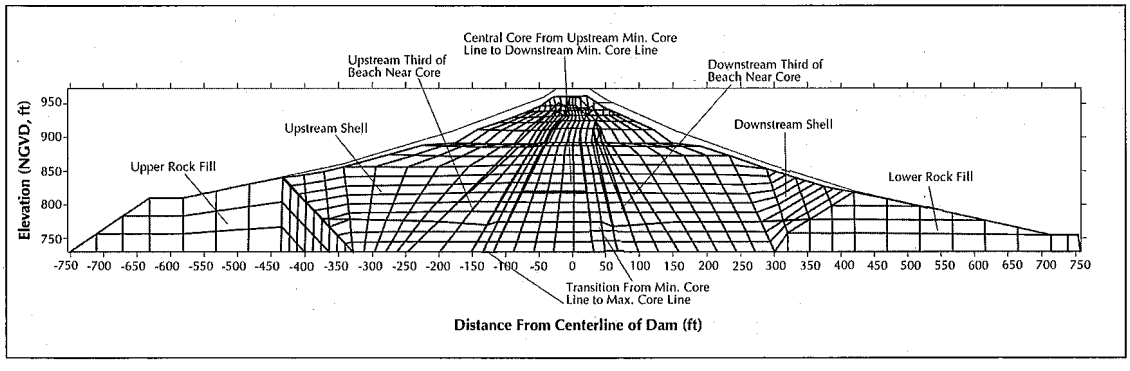

FIGURE 29. Deformed mesh (25-fold exaggeration), Cobble Mountain synthetic earthquake, QUAD-4M analysis, peak base acceleration 0.16 g, full pool, pseudo-three-dimensional analysis.

5- to 15-foot-thick layer of surficial crushed rock fill on the upstream slope. To evaluate these effects, this layer was modeled in two-dimensional QUAD-4M analyses for high and low pool levels using the Cobble Mountain synthetic record at 0.16 g. Computed factors of safety against liquefaction in the shallow areas along the upstream slope were at least 5.0. Figure 28 is one of the two design cases.

Figure 26 shows the settlement of the top surface corrected for three-dimensional effects. This figure is for the Cobble Mountain record and QUAD-4M analysis. It also includes the results for 0.12 g input.

Peak Base Acceleration – 0.204 g. The possible effects of an earthquake with a peak base acceleration of 0.204 g were investigated using the Chicoutimi-Nord earthquake record since

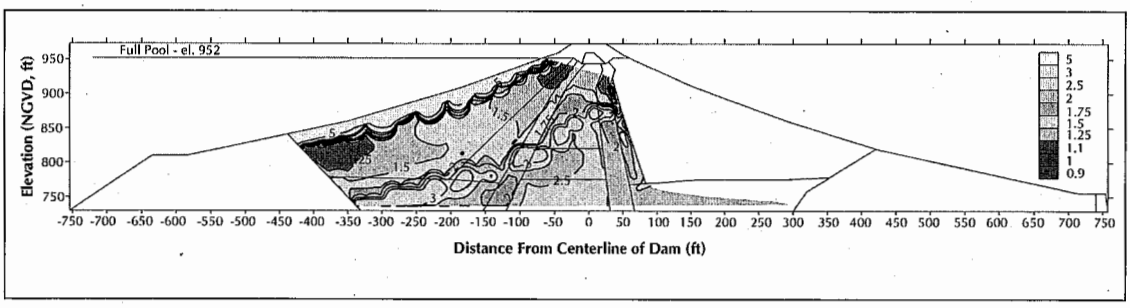

FIGURE 30. Factors of safety against liquefaction, Chicoutimi-Nord record, QUAD-4M analysis, peak base acceleration 0.204 g, full pool, upstream slope rockfill pseudo-three-dimensional analysis.

this record is judged to be more representative of the motions that could be expected from a synthetic earthquake record. Factors of safety against liquefaction, including three-dimensional effects and upstream slope rockfill, are plotted in Figures 30 and 31 for full pool and low pool, respectively. Figure 31 is the other of the two design cases. It contains a larger zone with the lowest range of factor of safety between 1.0 and 1.25 in comparison to the full pool case of Figure 30. When the upstream rockfill zone was not modeled initially the factor of safety for a significant size zone with the low pool cases was between 1.0 and 0.5. This result is entirely due to a modeling artifact. Figure 32 shows a typical deformed mesh for all cases, again with 25-fold exaggeration. Figure 33 shows the settlement of the top surface of the maximum section of the dam.

Conclusions

Liquefaction Potential. For the earthquake records and material properties considered in these analyses, there are adequate factors of safety against liquefaction throughout the central cross-section of the dam. The most severe case for the pseudo-three-dimensional analysis, which is judged to be the most appropriate for the geometry of this dam, occurs at low pool. Although three-dimensional considerations do affect the results (for example, somewhat reducing the factors of safety against liquefaction for the Chicoutimi-Nord record), the computed factors of safety remain adequate. When the upstream rockfill is included in the model, the pseudo-three-dimensional cases with full pool give factors of safety against liquefaction of 1.25 to 1.50 or larger for all cases within Material 4 (lower upstream and downstream shells) and Materials 1 and 9 (central core). From the exterior slopes of the dam inward towards the core, the computed factors of safety against liquefaction are at least 1.0 to 1.1, 1.1 to 1.25 and 1.25 to 1.5 within Material 5 (upper upstream shell), Material 3 (upstream and downstream one-third beach-

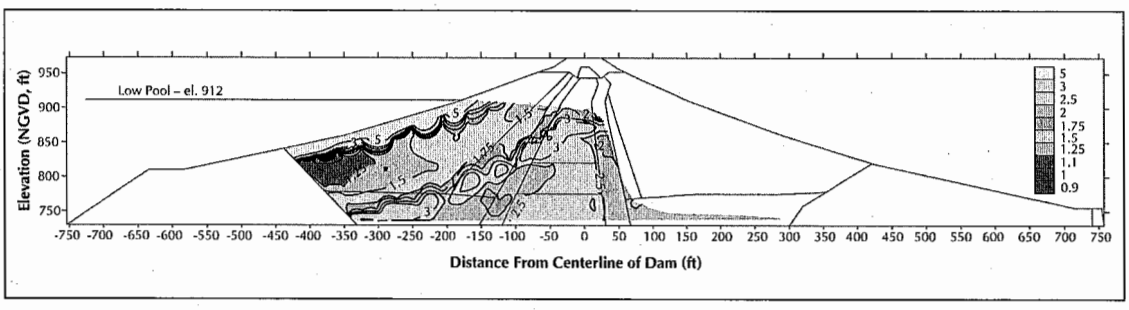

FIGURE 31. Factors of safety against liquefaction, Chicoutimi-Nord record, QUAD-4M analysis, peak base acceleration 0.204 g, low pool, upstream slope rockfill pseudo-three-dimensional analysis.

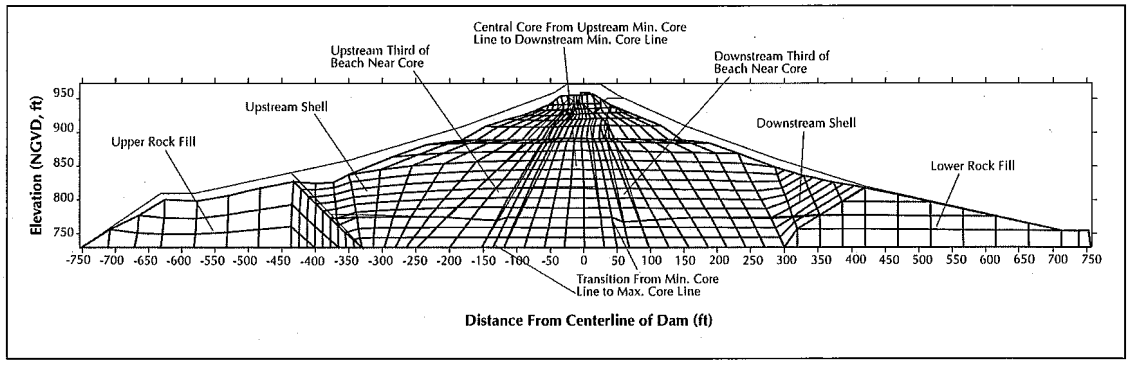

FIGURE 32. Deformed mesh (25-fold exaggeration), Chicoutimi-Nord record, QUAD-4M analysis, peak base acceleration 0.204 g, full pool, pseudo-three-dimensional analysis.

es) and Material 2 (upstream and downstream transitions), respectively. As would be expected, as the input acceleration increases, the factors of safety decrease.

Seismic Deformations. The estimated deformations of the dam under the seismic excitations are also acceptable. The most severe results are for an input peak acceleration of 0.204 g, which gives a maximum settlement of about 1.2 feet. In view of the many approximations in the analysis, it would be good practice to double this result, but the resulting settlement is still only approximately 2 feet. Also, it should be noted that the maximum settlement does not occur at the crest of the dam but at a point about halfway along the upstream slope surface. The computed crest settlement is in all cases less than 0.8 feet, which when doubled gives less than 1.6 feet, which correspond to small vertical strains on the order of 1 percent.

Impacts on Performance. The freeboard (vertical distance from dam crest to normal full reservoir pool) is 20 feet for this structure and it would not be compromised by deformations of the order of magnitude estimated from these analyses.

Analytical Procedures. These analyses employed six different finite element programs: SEEP/W, a proprietary flow program, SIGMA/W, QUAD-4M, FLUSH and PC-FEAP. The basic finite element mesh remained the same. Small, special-purpose programs

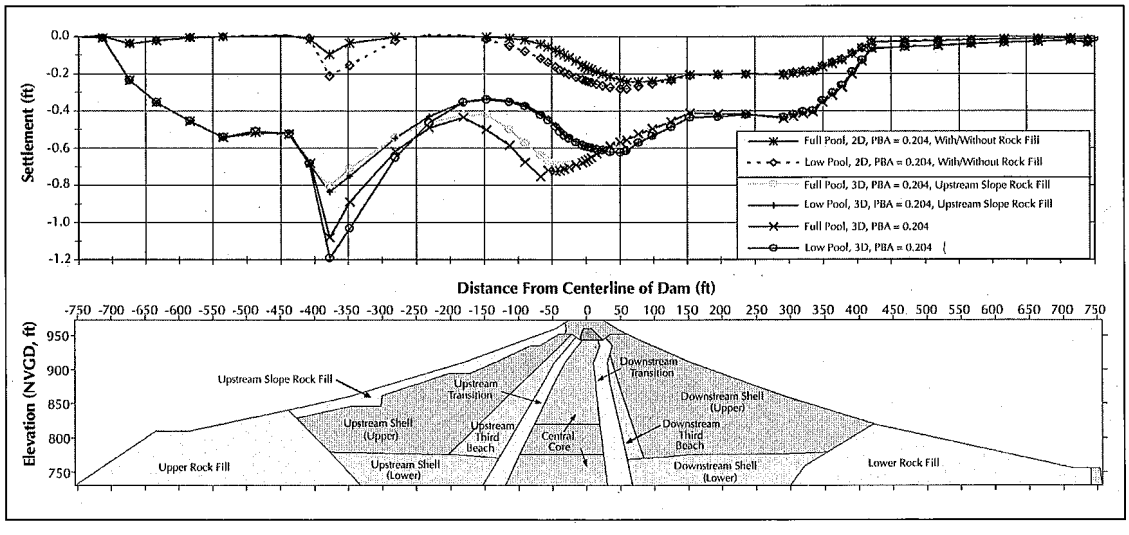

FIGURE 33. Estimated settlement along the top surface of profile, QUAD-4M analysis, Chicoutimi-Nord record, 0.204 g peak base acceleration.

were used to evaluate intermediate results, to compute local factors of safety or volume changes, and to pass data between the finite element programs. These programs worked element by element, preparing printed output, output suitable for plotting or output in appropriate format for input to subsequent finite element analyses. This approach had many advantages, including:

- using readily available, proven software;
- obtaining interim results, which could be studied to guide further analyses;
- eliminating the expense and delay of writing and debugging large new software; and,
- avoiding the rigidity of a large, canned program.

This approach does require that the analysts be able to access and to modify the input and output files for the various programs.

Presenting Results. The project engineers, the seismic response consultants and the client considered the analytical program a success. A major factor in this achievement was the presentation of results of the analyses in the form of color plots for a personal-computer-based presentation. In order to do so, the output from finite element programs was processed (without distortion) to accommodate the software needed to create the contour plots, plots of deformed meshes and plots of surface settlement. The results were well worth the effort.

ACKNOWLEDGMENTS —*The authors gratefully acknowledge the support of the Springfield Water and Sewer Commission (SWSC), John J. Lyons, Joseph J. Superneau, as well as the support of Anthony W. Curto and William S. Zoino. They thank Dr. Gonzalo Castro, of GEI Consultants, Inc., for his review of planning and work efforts of the project engineers. GZA GeoEnvironmental, Inc., of Norwood, Massachusetts, was engaged to perform the seismic response analysis. George Klimkiewicz and Vincent Murphy of Weston Geophysical Corporation performed the seismic hazard analysis in 2000. The seepage regime was evaluated using a proprietary finite element program developed by Prototype Engineering, Inc. The general-purpose finite element program PC-FEAP was developed by R.L. Taylor and is distributed by the National Information Service for Earthquake Engineering.*

ALFREDO URZUA *is the President of Prototype Engineering, Inc., in Winchester, Massachusetts. He received his Civil Engineering degree from the University of Chile, and a masters' degree and a Ph.D. in Civil Engineering from the Massachusetts Institute of Technology. He has over 25 years of experience in earthquake engineering, soil dynamics and numerical methods.*

JOHN T. CHRISTIAN, *Ph.D., P.E., has over forty years' experience in geotechnical engineering, including work on earth dams, finite elements, soil dynamics and earthquake engineering. He is an Honorary Member of BSCES, and Honorary member of ASCE and a member of the National Academy of Engineering. He will deliver the 38th Terzaghi Lecture in June 2003.*

WILLIAM H. HOVER, *P.E., is a senior principal and director of GZA GeoEnvironmental Technologies, Inc. He served as Principal-in-Charge of GZA's efforts on this project, and has evaluated many of the largest embankment and gravity dams and associated water supply systems and infrastructure in New England and New York.*

IVAN A. HEE *received a B.E. degree in Civil Engineering from Stevens Institute of Technology and a M.S. degree in Civil Engineering from Virginia Tech. He is currently employed as a geotechnical engineer with GZA GeoEnvironmental, Inc.*

STANLEY M. BEMBEN, *P.E. is a Professor Emeritus of the University of Massachusetts, Amherst. He received his B.S.C.E. from UMass, his M.S.C.E. from the University of Illinois and his Ph.D. from Cornell University. He is a consultant in geotechnical and forensic engineering and served as the lead project engineer for SWSC.*

REFERENCES

1. United States Army Corps of Engineers, *Phase I Inspection Report, National Dam Inspection Report, Cobble Mountain Dam (MA 00068) Russell, Massachusetts,* report prepared by New England Division, 1980.

2. Keyes Associates, *Municipally Owned Dam Inspection/Evaluation Report, Cobble Mountain Reservoir,* MA ID No. 1-7-256-11, report prepared for Commonwealth of Massachusetts, Department of Environmental Management, 1987.

3. Bemben, S.M., & Zoino, W.S., *Evaluation of Seismic Stability of Cobble Mountain Dam, Report to Springfield Water and Sewer Commission,* Vol. 1–3, December 4, 2000.

4. Bemben, S.M., Zoino, W.S., & Hover, W.H., "The Seismic Stability of Cobble Mountain Dam, Russell, Massachusetts," *21st Annual USSD Lecture Series,* Denver, Colorado, 2001.

5. Roald Haested, Inc., *Soil Boring,* report prepared for Board of Water Commissioners, Springfield, Massachusetts, 1989.

6. Hardin, B.O., & Black, W.L., "Vibration Modulus of Normally Consolidated Clay," *Journal of the Soil Mechanics and Foundations Division, ASCE,* Vol. 94, No. SM2, 1968.

7. Seed, H.B., & Idriss, I.M., *Soil Moduli and Damping Factors for Dynamic Response Analyses,* Report EERC 70-10, Earthquake Engineering Research Center, Univ. of California, Berkeley, 1970.

8. GEI Consultants, Inc., letter report of the *in-situ* shear wave velocity measurements, November 22, 1999.

9. Weston Geophysical Corporation, *Seismic Hazard Analysis: Cobble Mountain Reservoir Dam,* draft report to Springfield Water and Sewer Commission, 2000.

10. Tippetts, Abbett, McCarthy and Stratton, Inc., *Final Report – Dynamic Analysis of Knightville Dam,* prepared for U. S. Army Corps of Engineers, New England Division, 1982.

11. Geo-Slope International Ltd., *SIGMA/W, Version 4.21 documentation,* Calgary, Alberta, Canada, 1999.

12. Geo-Slope International Ltd., *SEEP/W, Version 4.23 documentation,* Calgary, Alberta, Canada, 1999.

13. Christian, J.T., "Flow Nets from Finite Element Data," *International Journal for Numerical and Analytical Methods in Geomechanics,* Vol. 4, No. 2, 1980.

14. Hudson, B.O., Idriss, I.M., & Beikae, M., *User's Manual for QUAD-4M,* Center for Geotechnical Modeling, University of California, Davis, 1994.

15. Lysmer, J., Udaka, T., Tsai, C.F., & Seed, H.B., *FLUSH: A Computer Program for Approximate 3-D Analysis of Soil-Structure Interaction Problems,* Report EERC 75-30, Earthquake Engineering Research Center, University of California, Berkeley, 1975.

16. Vucetic, M., & Dobry, R., "Effect of Soil Plasticity on Cyclic Response," *Journal of the Geotechnical Division, ASCE,* Vol. 114, No. 2, 1991.

17. Makdisi, F.I., Kagawa, T., & Seed, H.B., "Seismic Response of Earth Dams in Triangular Canyons," *Journal of the Geotechnical Engineering Division, ASCE,* Vol. 108, No. GT10, 1982.

18. Youd, T.L., & twenty others, "Liquefaction Resistance of Soils: Summary Report from the 1996 NCEER and 1998 NCEER/NSF Workshops on Evaluation of Liquefaction Resistance on Soils," *Journal of Geotechnical and Geoenvironmental Engineering, ASCE,* Vol. 127, No. 10, 2001.

19. Tokimatsu, K., & Seed, H.B., "Evaluation of Settlements in Sand Due to Earthquake Shaking," *Journal of Geotechnical Engineering, ASCE,* Vol. 113, No. 8, 1987.

20. Ishihara, K., & Yoshimine, M., "Evaluation of Settlements in Sand Deposits Following Liquefaction During Earthquakes," *Soils and Foundations,* Vol. 32, 1992.

21. Ishihara, K., *Soil Behaviour in Earthquake Geotechnics,* Oxford Science Publications, Oxford, Clarendon Press, 1996.

22. National Information Service for Earthquake Engineering, *NISEE CDROM Software Library,* University of California, Berkeley, Calif., 1998.